# Geosciences 2013

Annual Conference of the Geoscience Society of New Zealand. Christchurch.

## Field Trip 6

Thursday 28th November 2013

# Geomorphology, Structure and Interactions of the Canterbury Active Fault Network

Leaders: Brendan Duffy, Jarg Pettinga and Jocelyn Campbell

Department of Geological Sciences, University of Canterbury

**Cover photo**

Surface rupture on the Greendale fault. Photo Kate Pedley, University of Canterbury

**Bibliographic reference:**

Duffy, B., Pettinga, J.R. and Campbell, J. (2013). Geomorphology, structure and interactions of the Canterbury active fault network. In: Reid, C.M. & Hampton, S.J. (compilers). Field Trip Guides, Geosciences 2013 Conference, Christchurch, New Zealand. Geoscience Society of New Zealand Miscellaneous Publication 136B, 19 p.

ISBN 978-1-877480-34-8,
ISSN 2230-4487 (print)
ISSN 2230-4495 (online)

**Health and safety**

Participants need to be prepared for a wide range of environmental conditions (wind, cold, heat, etc). We will be travelling a long distance and you won't have an opportunity to return for extra layers. Bring sunhat, sunblock, parka, an extra warm layer and sturdy footwear. Hammers will not be required. Most stops will be roadside so please be aware of traffic.

**Itinerary**

| | |
|---|---|
| 8.15am | Meet at UC Science carpark |
| 8.30am | Depart UC Science carpark |
| 8.30-9.15am | Travel to Highfield Road |
| 9.15-9.50am | Stop 1 and 2 - Highfield and Telegraph Road |
| 9.50-10.15am | Travel to Ridgens Road switching station |
| 10.15- 11.15am | Stop 3 and 4 – West segment Greendale fault |
| 11.15-11.40am | Travel to Sheffield |
| 11.40am -12.00pm | Purchase lunch and drive to Waimakariri Gorge |
| 12.00pm-12.40pm | Stop 5 – Lunch Waimakariri Gorge |
| 12.40pm-1.30pm | Travel to Cust/Springbank |
| 1.30pm-2.45pm | Stop 6 – Springbank and Cust structures |
| 2.45pm-3.10pm | Travel to Ashley fault |
| 3.10pm-4.30pm | Stop 7 – the Ashley and Loburn faults |

## Introduction

Over the last decade, technologies such as InSAR (e.g. Reigber et al., 1997; Price and Burgmann, 2002; Beavan et al., 2010) and LiDAR (e.g. Hudnut et al., 2002; Quigley et al., 2012; Duffy et al., 2013) have increasingly supplemented well-established field methods, including geological/geomorphic mapping and geodetic surveying, during documentation of fault surface rupture. In combination, these methods have provided exceptional opportunities for examining active drivers of ground surface deformation and kinematics in unrivalled detail and precision. Compared with surface rupture documentation, the detection of unrecognised faults in alluvial settings similar to Canterbury has always been challenging, and has usually involved careful analysis of fluvial planforms, profiles and depositional settings (e.g. Holbrook and Schumm, 1999). LiDAR has provided a welcome boost to these efforts, particularly where it is used in conjunction with geophysical techniques (e.g. Gold et al., 2013). In Canterbury we now have an opportunity to further our understanding of the Canterbury seismic hazard, by documenting the history of the Greendale fault system, refining our understanding of the geomorphic and sedimentary signature of deformation, and using these as a guide to detecting 'new' and/or previously-undetected faults. During this field trip we will visit key known components of the Canterbury active fault network. We will focus on their roles in accommodating plate boundary deformation, by evaluating their geomorphic expression, structure and interaction. We will discuss directions for further research, and the best ways to target our efforts in the wide open plains.

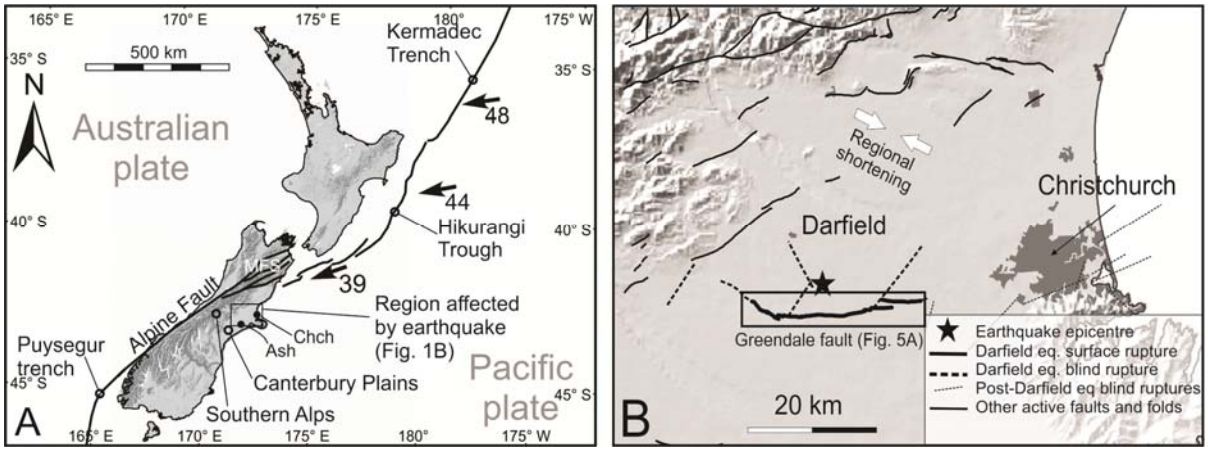


***Figure 1.*** *Regional setting. A) New Zealand plate boundary and relative motion vectors (mm/yr) between the Australian and Pacific Plates (DeMets et al., 2010). Canterbury Plains form the low relief region east of the Southern Alps in the central South Island. Ash – Ashburton; Chch – Christchurch. B) Location of the Greendale fault west of Christchurch in mid-Canterbury. The extent of surface rupture is from Quigley et al. (2012), and extents of blind ruptures are from Beavan et al. (2012). Known active (i.e. late Quaternary) faults and folds are based on GNS Science QMAP datasets (Cox and Barrell, 2007; Forsyth et al., 2008). Regional shortening direction from Sibson et al. (2011).*

### *Geological background*

The Marlborough fault system (MFS) of the northern South Island transfers slip from the Hikurangi subduction system to the Alpine fault and is propagating southward (Little and Jones, 1998) (Figure 1). Back-thrusting in relation to the Alpine fault creates a southeasterly-advancing, repetitive structural pattern in Canterbury that is dominated by the propagation of northeast-striking thrust assemblages (Figure 2). Plate boundary deformation in the Canterbury area therefore reflects both the eastward propagation of these backthrusts with respect to the Alpine fault, and the southward

propagation of the MFS. The pattern of thrusting is regularly segmented by east-west faults inherited from Cretaceous/Paleogene normal faults developed on the Chatham Rise (Wood and Herzer, 1993), which are now being re-activated in transpression (Nicol, 1993; Ghisetti and Sibson, 2012). The east-west faults act as tear faults that transfer relative motion between thrust segments and accommodate oblique transpressive shear (Figure 2). The early stages of thrust emergence are dominated by anticlinal growth and blind, or partially buried, thrusts and backthrusts. Rupture on connecting east-west faults therefore record timing of coseismic episodes of uplift and shortening on their partner thrusts. This results in variable horizontal to vertical slip ratios that reflect displacement on the hidden adjacent thrusts (Campbell et al., 2012). These fault systems are well-documented close to the rangefront, and the inherited structure is well-known offshore (Wood and Herzer, 1993). However, active faulting is poorly resolved in onshore areas with poor seismic reflection coverage (Jongens et al., 2012) (Figure 3)

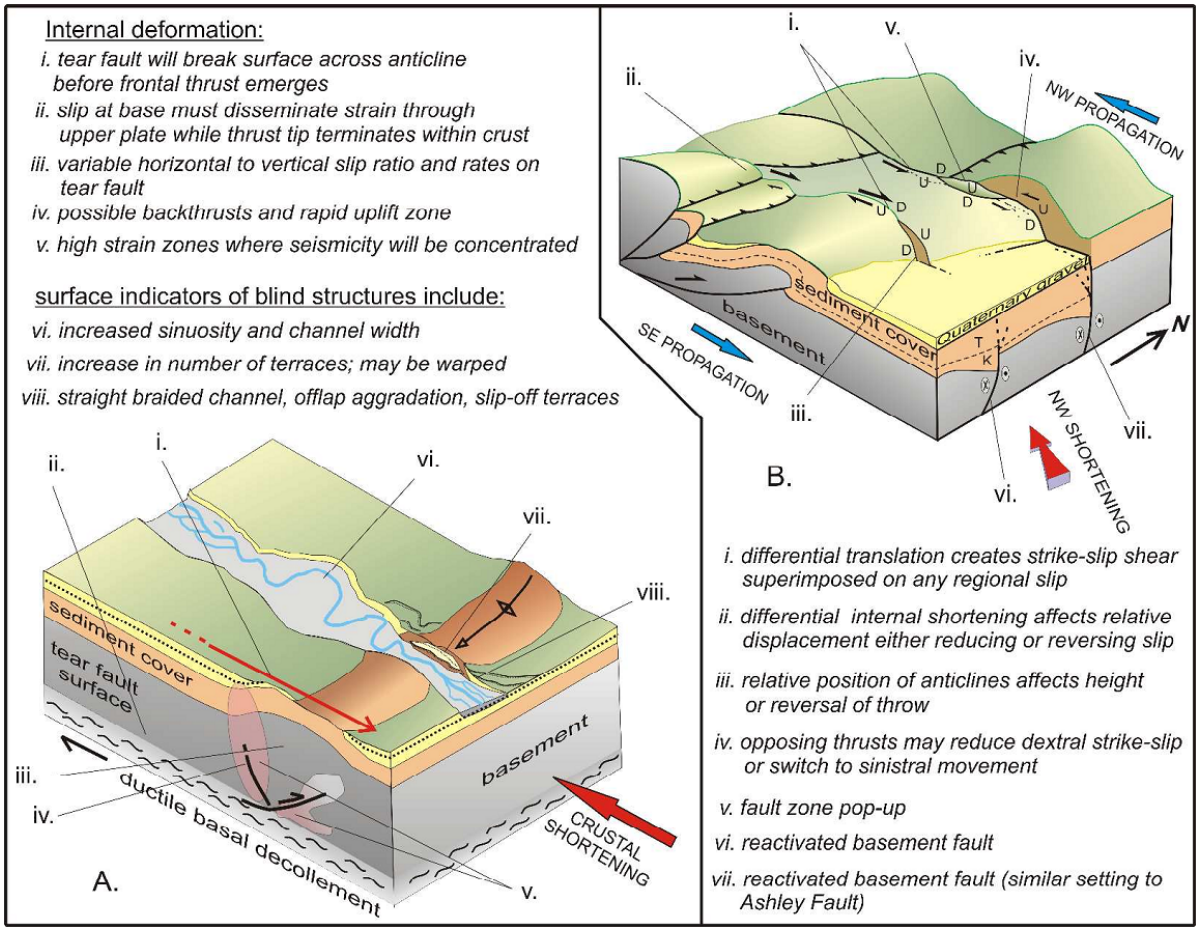


***Figure 2.*** *From Campbell et al. (2012). A: Block diagram showing the internal distribution of strain associated with a blind thrust and the surface response of antecedent drainage and landforms. The left-hand face of the block diagram represents a tear fault surface ideally perpendicular to the blind thrust. B: Block diagram showing east-west striking reactivated basement faults intersecting a northeast-striking thrust fault and fold system. Schematically this shows how relative rates of translation and the distribution of internal shortening by folding can modify the slip distribution along transecting faults. The size of the movement arrows on transecting faults is proportional to the amount of relative slip. T = Tertiary rocks, K = Cretaceous rocks. U= Up, D = Down.*

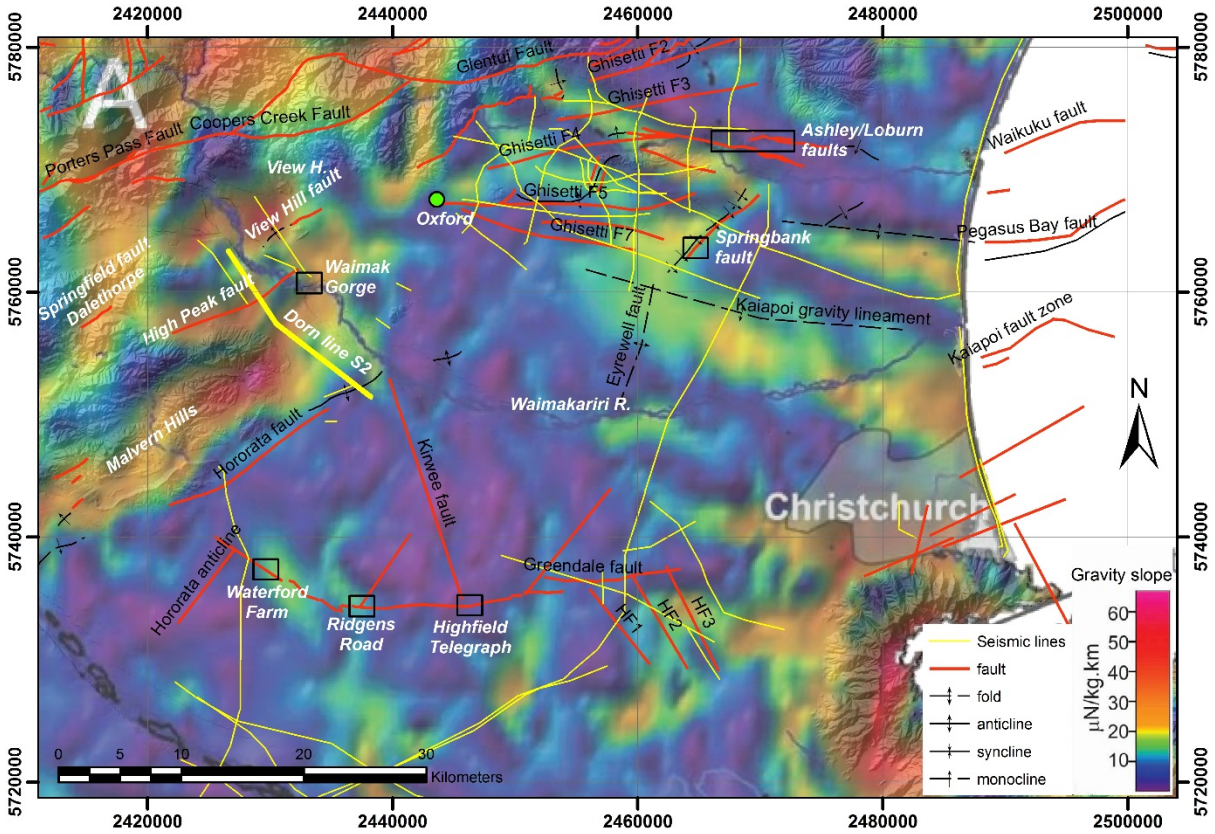


***Figure 3.*** *Central Canterbury showing field trip localities (black rectangles). Base is a Bouguer anomaly slope map (Davy et al., 2012) overlaid on a digital elevation model of North Canterbury. The base is overlaid with mapped faults and folds and published seismic lines. Faults are from the Christchurch QMap (Forsyth et al., 2008), modified after Ghisetti and Sibson (2012). Faults labelled Ghisetti F… are reactivated faults interpreted by Ghisetti and Sibson (2012), based on industry seismic. Central Canterbury (north of the Greendale fault and south of the Eyre River) is notably deficient in both mapped faults and seismic reflection surveys and gravity slope lineaments provide the main indication of fault density in that area.*

## *The Canterbury earthquake sequence*

South-east of the rangefront, slip rates are low (Wallace et al., 2007), and rupture timescales are long compared with the rates at which the Canterbury Plains are resurfaced (Brown et al., 1988). Much of the deformation is hidden under and within thick Quaternary alluvium. Within this setting, the $M_w$ 7.1 Darfield earthquake centred 40 km west of Christchurch on 4$^{th}$ September 2010 initiated an energetic aftershock sequence (Figure 4) that has included three other earthquakes >Mw6, including the 22$^{nd}$ February 2011 earthquake that destroyed much of Christchurch's central business district. Overall, the Canterbury earthquake sequence has now caused rupture on more than eleven faults including up to 7 in the initial earthquake event (Beavan et al., 2012; Elliott et al., 2012; Syracuse et al., 2013). One striking aspect of the earthquake sequence that accompanied and followed the ground rupture has been the complex association of blind thrusting with strike-slip faulting, in keeping with observations of Canterbury's structural style (Campbell et al., 2012) (Figure 2). Both the Darfield and Christchurch earthquakes were triggered by thrusting that propagated into strike-slip displacements on dominantly E-W faults (Gledhill et al., 2011; Elliott et al., 2012; Kaiser et al., 2012). Ground rupture only occurred on strike-slip faults, whilst all thrust faults remained blind.

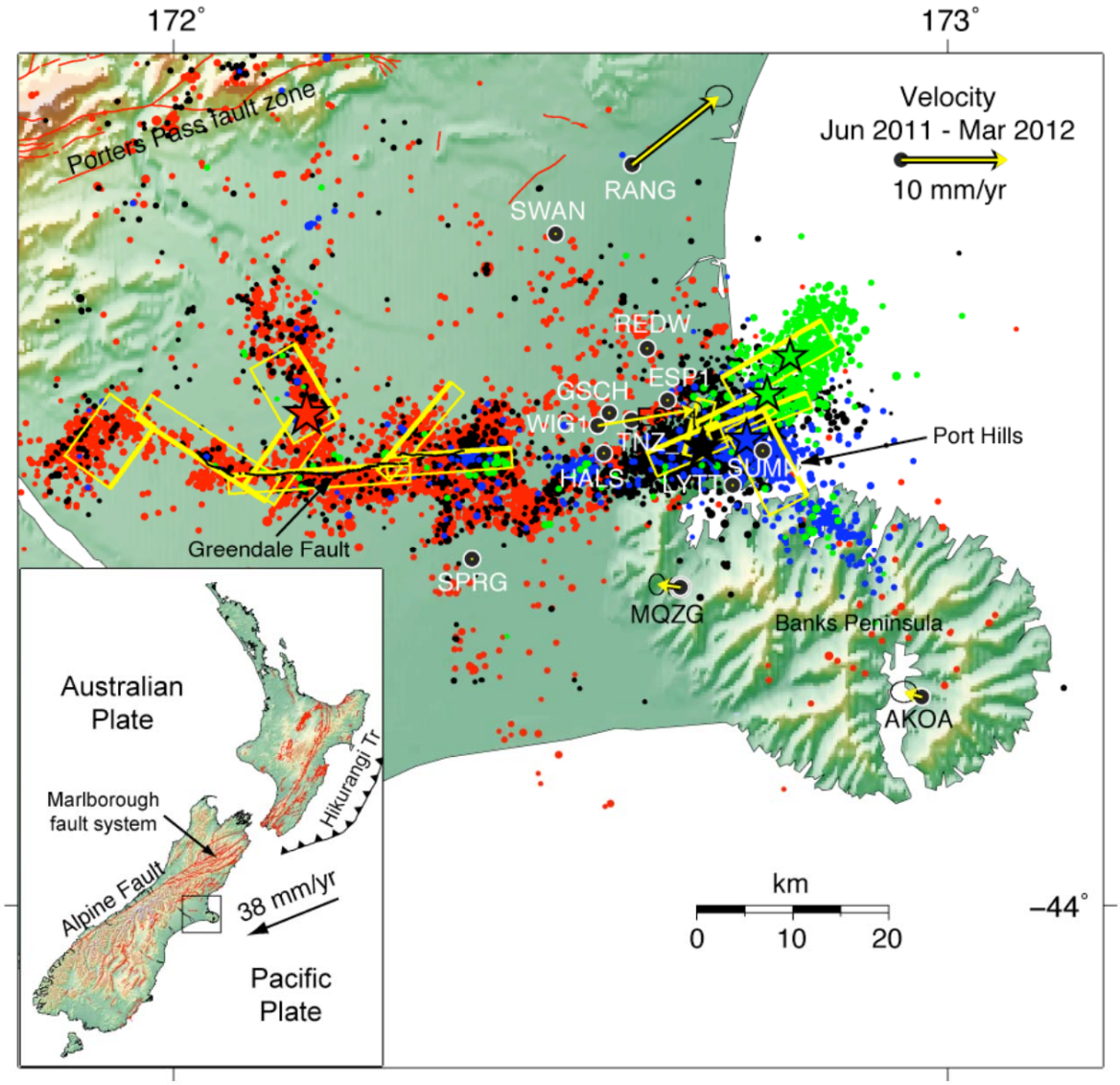


***Figure 4.*** *(From Beavan et al., 2012) Epicentres, aftershocks and modelled fault planes for the 2010-present Canterbury earthquake sequence. Mainshocks (stars) and aftershocks (points) are colour-coded as follows: Red – 4 Sept 2010; Black – 22 Feb 2011; Blue – 13 June 2011; Green – 23 Dec 2011.*

The surface rupture on the east-west striking Greendale fault has since been examined and documented in a level of detail that is globally unprecedented (Figure 5) (Quigley et al., 2012; Duffy et al., 2013). High resolution displacement data indicate that the fault had a surface rupture length that was up to 50% shorter than other strike-slip earthquakes with similar displacement characteristics (Figure 6). Campbell et al. (2012) interpreted these high strain rates as resulting from transfer of displacement between NE-striking thrusts by reactivation of E-striking Cretaceous/Paleogene normal faults. This mechanism is particularly well documented in the Waipara area, where the Boby's Creek fault links the Grey and Karetu thrust faults, and rupture on these linked faults appears to have been synchronous (Nicol and Campbell, 2001). The Boby's Creek fault has an apparently shorter surface rupture length (9 km) and a similar single-event displacement (5 m) to the Greendale fault (Figure 6). This high ratio of displacement to rupture length appears to set Canterbury E-W strike-slip faults apart from other strike-slip earthquakes around the world.

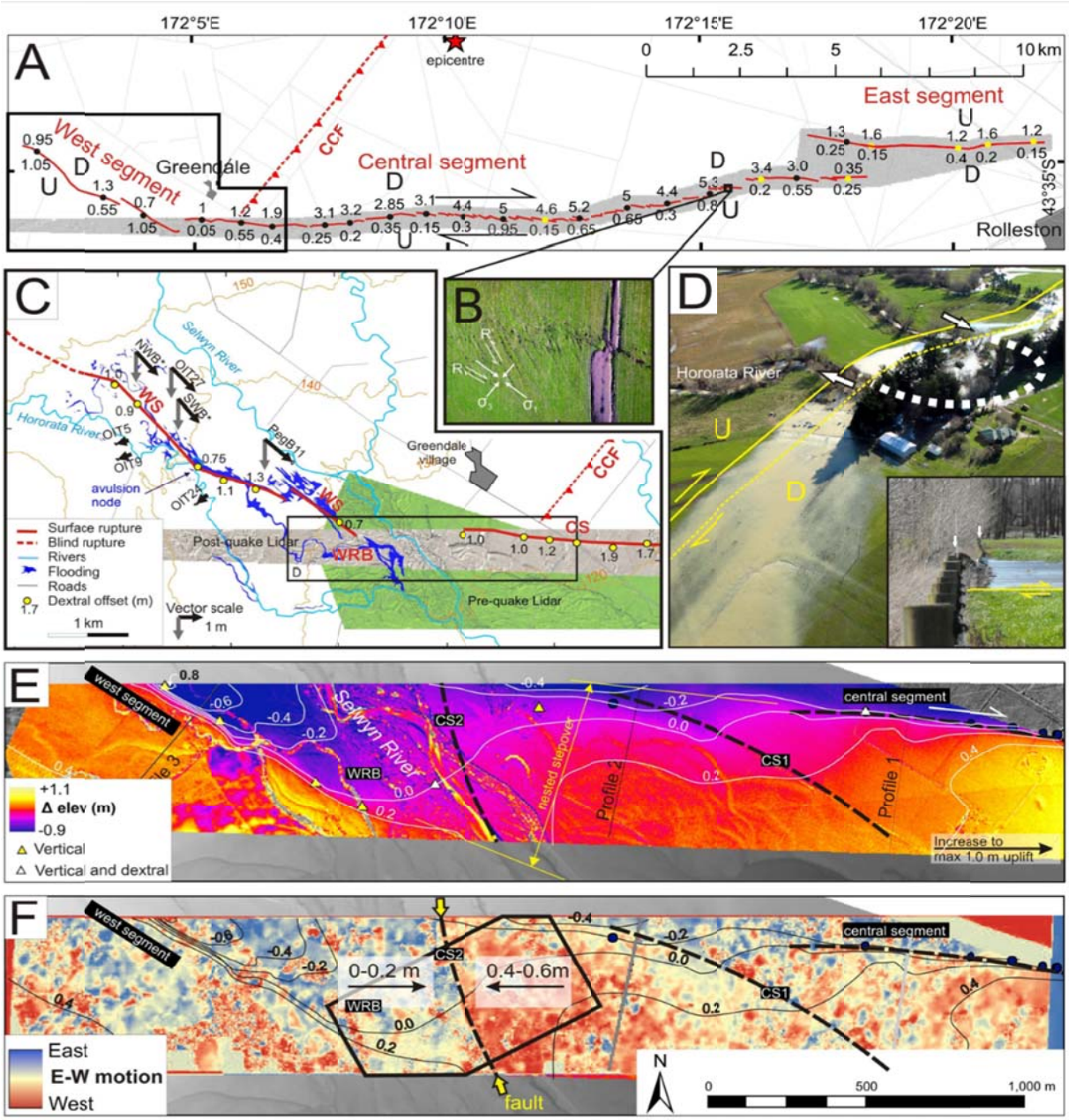


***Figure 5.*** *A) offset details along the segments of the Greendale fault trace: Annotations provide strike-slip displacements on north side, vertical displacements on south. B) Interpretation of shear pattern east of Highfield Road. C) West Segment wall rock displacement vectors from GPS, cadastral data and differential LiDAR coverage. D) Disruption of a meander bend in the bed of the Hororata River, and consequent flooding. E) Differential LiDAR analysis of changes in elevation at the junction of the central and West segments of the Greendale fault. Note zone of compression and uplift between oblique faults CS1 and CS2. F) Horizontal components of motion across the junction from Cosi-Corr analysis of LiDAR. Note convergence across CS2. Figure compiled from Quigley et al. (2012) and Duffy et al. (2013).*

In addition to surface rupture, studies following the Canterbury earthquake sequence (CES) have provided a wealth of (sometimes-contradictory) geophysical and seismological evidence for active faulting in the basement of the Canterbury plains. (Davy et al., 2012; Syracuse et al., 2013). These faults clearly interact in a complex way, but the surface expression of many of these faults and their zones of interaction remains indeterminate at depths beneath the plains. The Canterbury active fault network is still poorly defined. Areas with dense seismic survey lines typically have a much greater

density of mapped faults than areas with poor seismic coverage (e.g. Jongens et al., 1999; Ghisetti and Sibson, 2012; Jongens et al., 2012) (Figure 3), especially when compared with offshore mapped faults (Barnes et al., 2011).

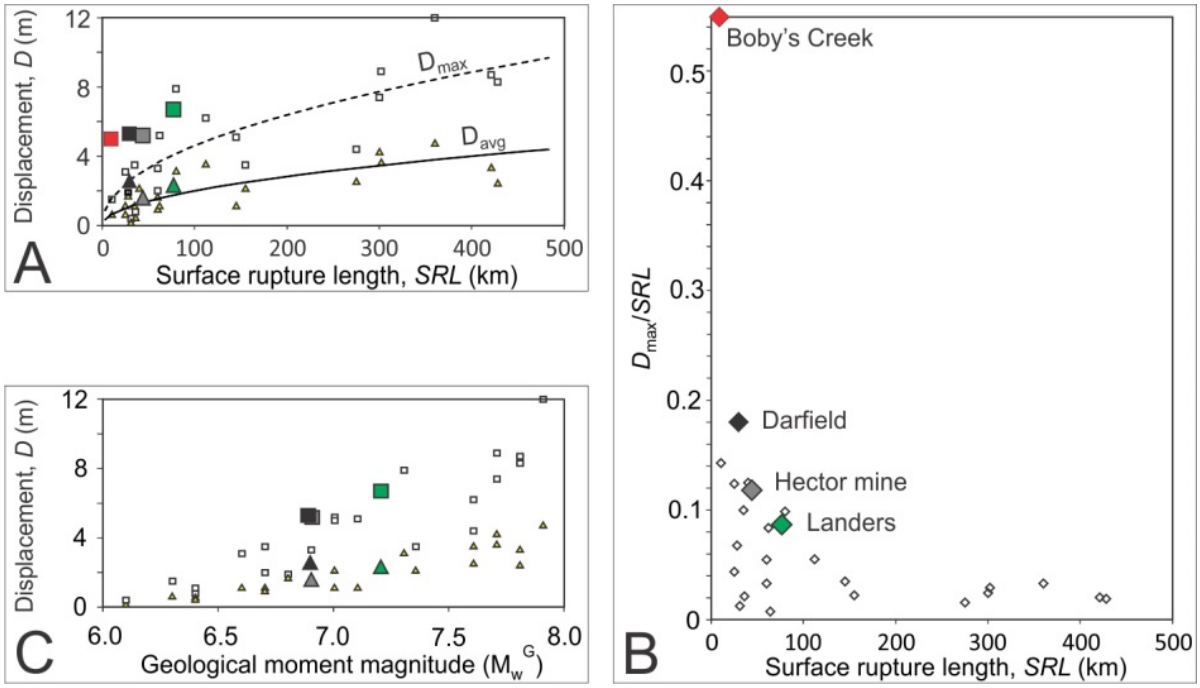


Figure 6. (modified from Quigley et al., 2012) Rupture scaling relationships for large strike-slip earthquakes (open symbols), specifically including the Darfield (black symbols), Landers (green symbols), and Hector Mine earthquakes (gray symbols), and paleoseismic data from the Boby's Creek fault. Note the high displacement compared with the short rupture length for E-W Canterbury strike-slip faults.

## The Greendale fault

### Highfield Road/Telegraph Road (stop 1 and 2)

The earthquake took place at 4:35 am and by 9:30 am. a team from the University of Canterbury had located the ground rupture. They were greeted by maintenance workers already repairing the road, which was offset by 5m of dextral strike-slip (Figure 7A). The en-echelon pattern of left-stepping Riedel shears was immediately obvious where the rupture passed through a small patch of forest[1] (Figure 7B). The forest was quickly felled by a NW wind within days of the earthquake.

The earthquake team's focus quickly shifted to Highfield Road, the supposed next job of the road repair team (Figure 7C). That site was secured and preserved for several days after the earthquake. The spring season meant that much of the land around Highfield Road was either in short pasture or cultivation (e.g. Figure 7D), showing up the fine detail of the shear zone structure and offset markers such as roads and fences (e.g. Figure 5). Priority was given to putting this shear zone information on record.

Hornblow et al (in prep) have since excavated a trench across the Greendale fault immediately east of Highfield Road. The results will be available for discussion on the day.

[1] http://www.youtube.com/watch?v=lQMPN7e1r54

A

B

C

D

***Figure 7.*** *A: A road gang repairs Telegraph Road at ~9.30 on 4 September 2010. Bulging and shearing had already been repaired and the road opened shortly after. B: Offset tree rows immediately west of Telegraph Road. C: Shearing and bulging of Highfield Road (view to S). D: Mark Quigley stands on crop rows warped and offset by the fault trace west of Highfield Road.*

## Hororata/Greendale structures

### Ridgens Road substation (stop 3)

Approximately 600 m west of the intersection of Ridgens Road and Coaltrack Road, and about 200 m north of the Greendale fault, we cross the surface projection of the blind Charing Cross fault (Beavan et al., 2012) (Figure 8A). Unpublished differential LiDAR across this intersection clearly shows bulging of both the north and south sides of the Greendale fault across this intersection (Figure 8B). On the north side of the Greendale fault this results in a transition from net subsidence to net uplift of the ground surface (Figure 8C). We will stop at this locality and discuss the structural significance of bulging on both sides of the Greendale fault, and also the potential for documentation of previous interactions of these two faults at this locality.

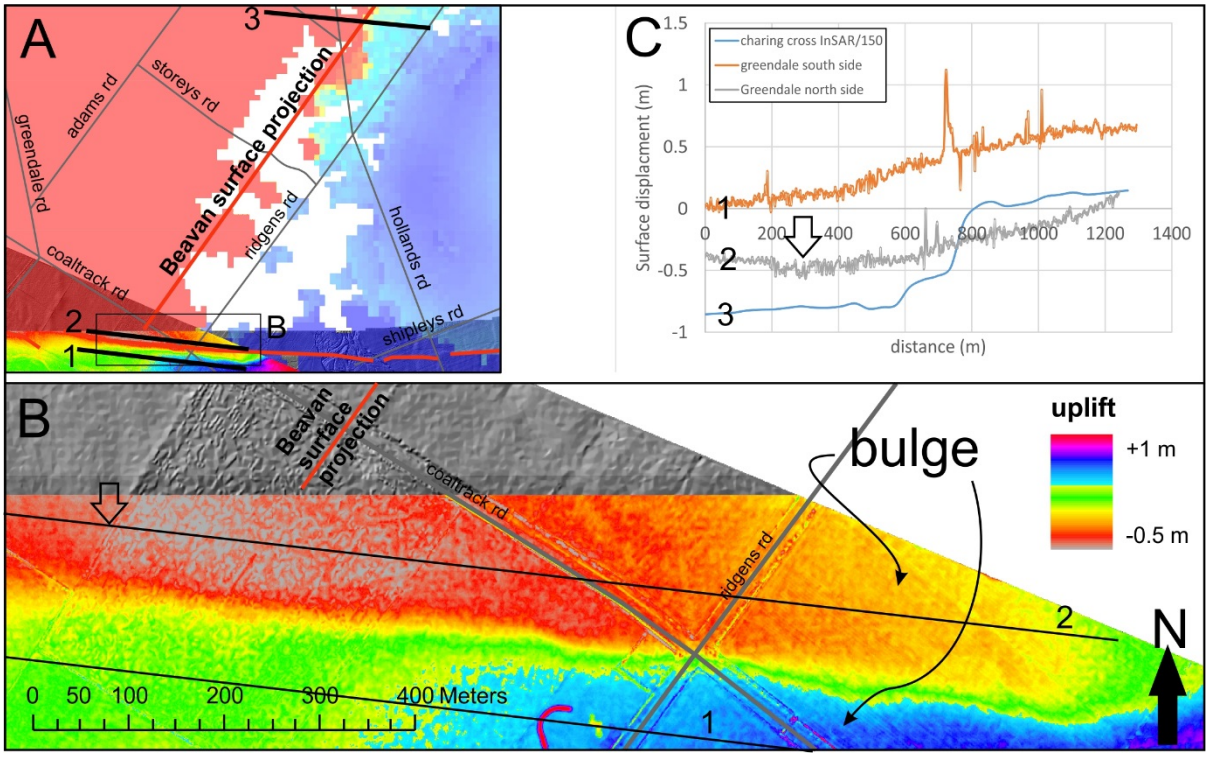


Figure 8. A) Differential LiDAR (2008 Selwyn minus 2010 quake) overlaid on unwrapped InSAR (courtesy of the late John Beavan). B) detail of the rectangular area outlined in A), showing bulging of the ground surface north and south of the Greendale fault. Bulging occurs immediately east of the surface projection of the Charing Cross fault favoured by Beavan et al. (2012). C) Profiles across the differential LiDAR (1&2) and Beavan's InSAR (3) The arrow on profile 2 is located at the position shown in B.

### The West segment (stop 4)

The West segment of the Greendale fault zone swings to a NW strike, geometrically forming a releasing bend for the slip on the Central segment. Aerial reconnaissance by GNS Science scientists tracked the western extent of the rupture and provided an immediate photographic record, also documenting avulsion of the Hororata River from its breached channel (Figure 5D). The photographic record of the avulsion was critical in establishing the location of the fault trace along the West Segment, where the trace paralleled pre-existing terraces (Barrell et al., 2011; Duffy et al., 2013) (Figure 5C). Nevertheless, the intersection of the Central and West segments of the Greendale

fault was an area of diffuse warping and low net slip, that was only clearly mapped using differential LiDAR and indicates a more complex structure and kinematic pattern than a simple releasing extension (Figure 5E&F) (Duffy et al., 2013). The northern wall rocks move towards a restraining bend at the step over between the West and Central segments, and shortening is taken up by two oblique-transpressive faults (Figure 5E&F). The southeast dipping Charing Cross thrust fault also projects under the intersection of the West and Central segments and overthrusts the West segment hanging wall. Beyond the surface rupture, the West Segment projects west to intersect the frontal structures of the northeast striking Hororata thrust fault zone that fronts the Malvern Hills. There, the Hororata Anticline is shown in a seismic reflection section to be propagating on the leading edge of a blind footwall thrust (Jongens et al., 2012). It is not surprising that this site of multiple fault interaction and stress loading was an important location in the complex rupture triggering process.

### Sheffield & Springfield structures (stop 5 and lunch)

Basement is exposed in the hanging wall anticline of the Hororata fault, forming the fold and thrust-generated topography in the Malvern Hills. The basement exposure is partly due to removal of the thin cover of Tertiary sediments that overlie over the original basement high on the inland extension of the Chatham Rise. These sediments thicken north of the Malvern Hills, suggesting that an E-W fault lies immediately north of the Malvern Hills (see Figure 3 for possible lineaments), but the same thrust fault system projecting into the basin under the Waimakariri River shows fault displacements of comparable amplitudes in seismic reflection lines (Dorn et al., 2010). In places the (thicker) Tertiary sequence is uplifted above the Quaternary gravels of the Plains and, in some cases, as at the Waimakariri Gorge, basement is exposed.

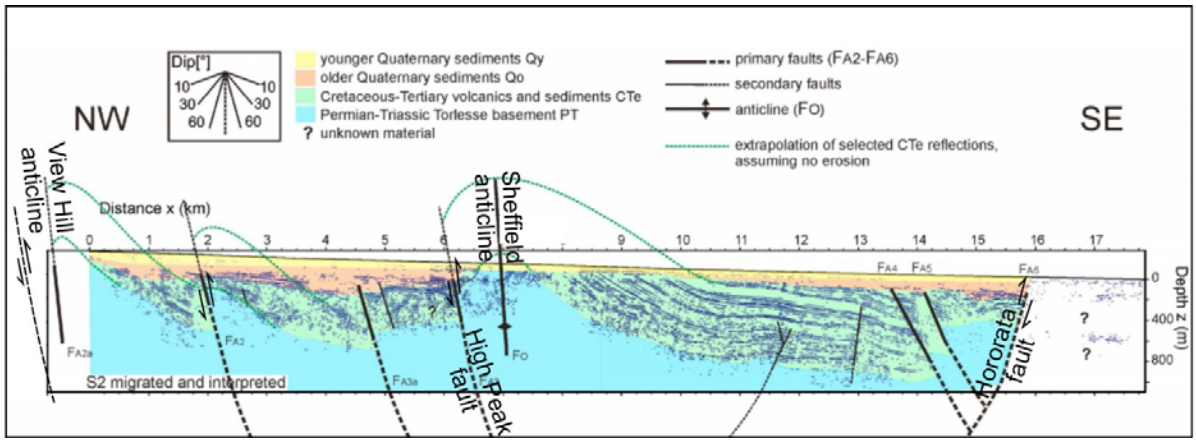


*Figure 9. Interpreted seismic reflection line on south bank of Waimakariri River (Dorn line S2 on Figure 3). The unknown material to the SE (marked ?) is probably predominantly gravel with some weak reflectors, but it is not possible to differentiate identifiable units, suggesting that the Hororata fault has been disrupting the geological fabric of the footwall over a considerable distance (Dorn et al., 2010, modified from their Fig.10).*

We will visit the Sheffield pie shop for those of you that don't have a packed lunch and, weather permitting, will eat at the Waimakariri Gorge. From the south side of the Waimakariri River the road crosses the river at the gorge where the river is incised into Torlesse greywacke basement brought to the surface in the core of the Sheffield anticline. This is on the hanging wall of the High Peak Fault (Figure 9). Approximately ~400m of Quaternary gravel is incorporated in the footwall syncline compared with a total throw of 500m on the main fault plus splays, implying that much of the

displacement is mid to late Quaternary. Additionally there is 400m of amplitude on the leading edge anticline on the hanging wall near Sheffield (Figure 9). On the north side of the river, the dip slope of volcanics on View Hill can be seen further to the the west, a similar anticline on a strand of the Springfield fault zone just off the NW end of Figure 9.

### Cust/Springbank structures (stop 6)

Elements of both the northeast-striking thrust system and east trending reactivated inherited structures are present along the western and northern margins of the Canterbury Plains. The availability of a more comprehensive coverage of late 1990's industry seismic reflection lines in this area (e.g. Ghisetti and Sibson, 2012; Jongens et al., 2012) (Figure 3) shows that these displacement transfer structures are more evolved, but similar in style, to the Hororata-Greendale-Charing Cross system and related faults.

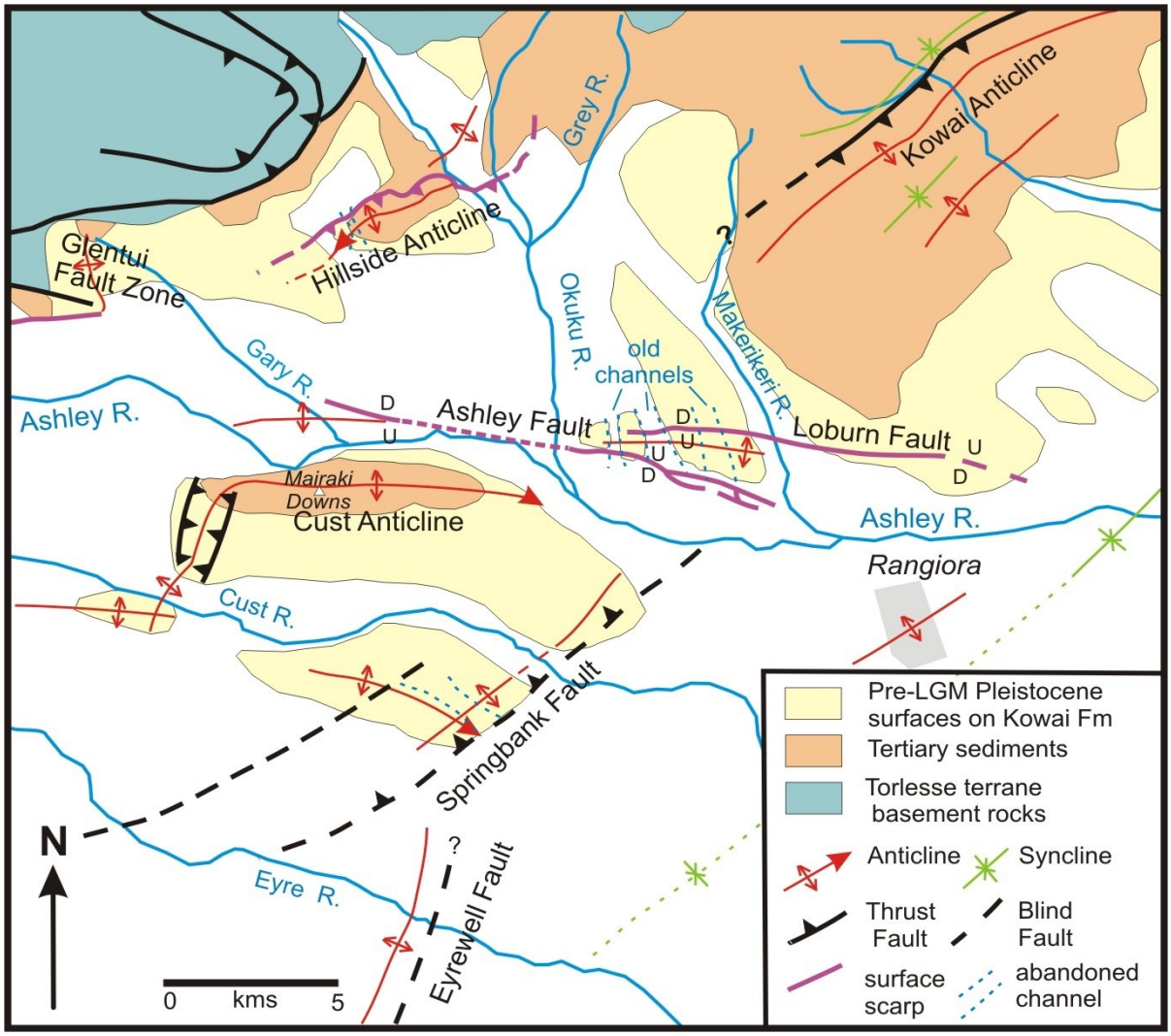


***Figure 10.*** *Generalized geological map of northern Canterbury Plains showing major structures and rivers (Campbell et al., 2012). All the area shown in white is outwash gravel from the peak of the Last Glacial Maximum (LGM) and subsequent degradation and reworked surfaces to the modern channels.*

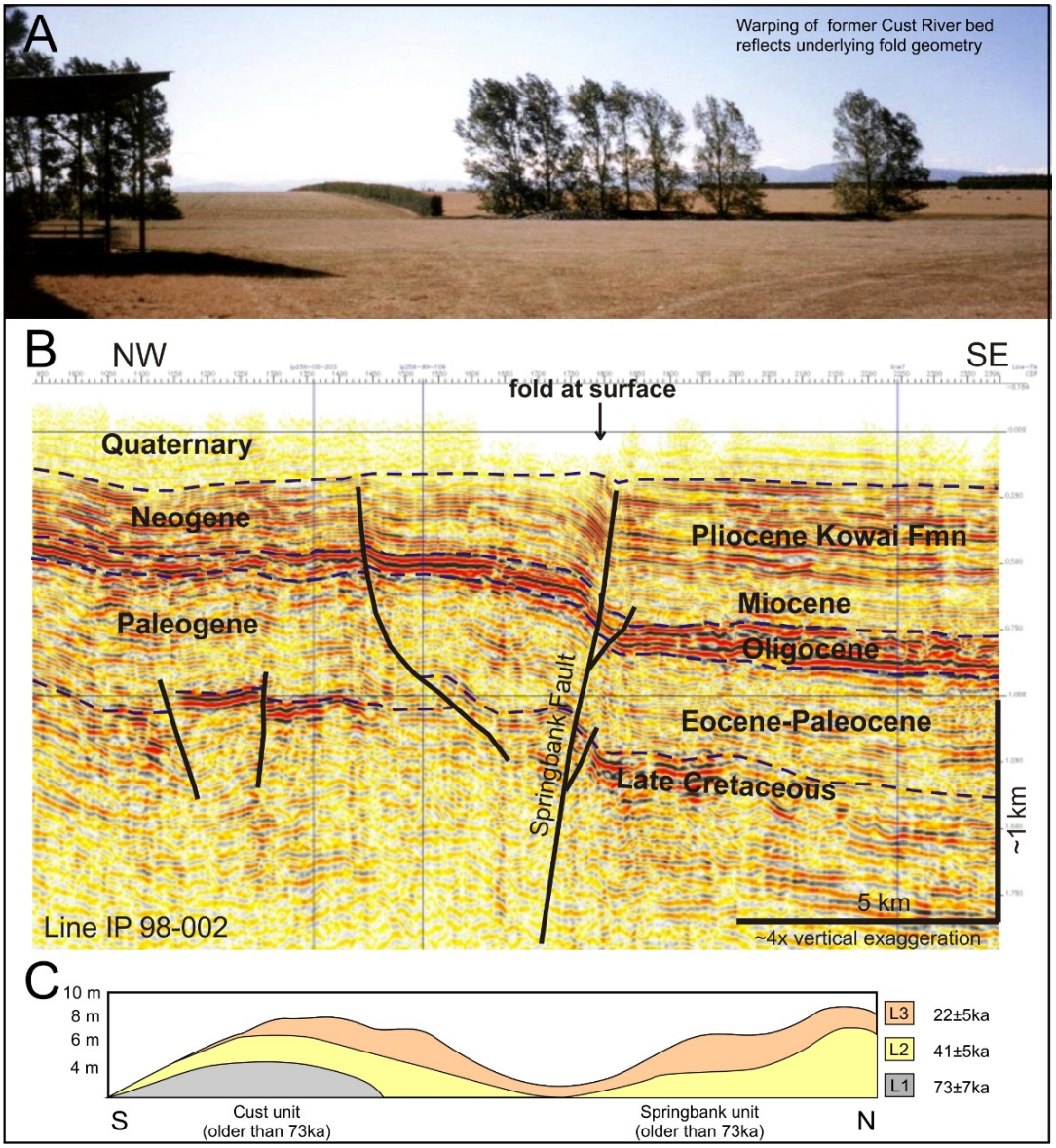


***Figure 11.*** *The Springbank blind thrust and associated folding. A: View to NW of the forelimb of the thrust-propagation anticline. The curved surface is the former bed of the Cust River preserved above a late Pleistocene aggradation surface (photo by J. Campbell). B: Industry seismic reflection line along Tram Road, crossing the Springbank fault-propagation fold structure, and showing an associated backthrust (Jongens et al., 2012). C: Dated loess profile on the crest of the Springbank structure. The former course of the Cust River occupied the central depression. Early loess deposition (OIS 4) is preserved on the south side but is stripped by the river eroding into uplifting Kowai gravels. During OIS 3, the central channel was being abandoned upstream of this section and the river migrated and downcut to the present channel. This was followed by deposition of the regional loess during the LGM (OIS 2). (dates from Berger et al., 2001 in Estrada, 2003)*

### *The Springbank fault*

A well-documented example on the low downlands south of the Cust River relates to the nearly emergent blind thrust of the Springbank Fault (Figure 10). Our route follows the north side of the Eyre River and eventually turns north to approach the Springbank structure from the south and east (Figure 11A). The Springbank Fault strikes NE and dips NW and is imaged in an industry seismic reflection line along Tram Road (Jongens et al., 2012) (Figure 11B). Paleogene reflectors at depth are clearly disrupted, and the eastwards-thickening of Miocene sediments across the fault suggests that

slip initiated in the Miocene (Jongens et al., 2012). Pliocene Kowai Formation is strongly folded but only slightly disrupted, whilst near-surface reflectors are only monoclinally folded. The overall structure forms a box anticline on the hanging wall of the Springbank fault. The eastern limb is a monocline that parallels the topography of a rounded scarp, across which the topography steps up abruptly by ~50 m, from the Canterbury Plains to the Cust downlands (Figure 11A). The smooth, rounded surface seen in this image is the now-folded former bed of the broad, braided Cust River, which then included the former course of the Ashley River (Campbell et al., 2012).

The Springbank blind-thrust propagated fold structure emerged above the erosion level within the period of the Last Glaciation (Estrada, 2003). Incision of this paleo-channel across the crest of the fold preceded a history of slip-off to the north, which is documented by the loess stratigraphy on the abandoned surfaces (Figure 11). At some point the Ashley River switched to the north side of the L-shaped Cust anticline, joining the Okuku River and leaving an underfit Cust River in its present channel (Figure 10).

The Springbank fault appears to terminate rather abruptly southwards before the Eyre River, and Estrada (2003) proposed the existence of the Eyrewell fault as a similar, buried, less evolved, fault further to the south. We will discuss the evidence for the Eyrewell fault, and whether an E-W fault picked out by gravity lineaments (Figure 3) may in fact define the southern limit of the Springbank fault.

## Ashley/Loburn fault system (stop 7)

### The Cust Anticline

Between the Cust and Ashley Rivers, the Cust Anticline forms a long ridge rising westward to a culmination of 140m above the river level. Here the fold turns abruptly southward at the intersection with uplift associated with backthrusts off the Springbank structure (Figure 10 and Figure 11). The abandoned broad channel of the original river system is eroded into this rising barrier, leaving only the incised remnant of the Cust River. Kowai Formation strata are exposed on the crest of the fold; younger onlapped gravels are preserved on the lower flanks with a thick loess blanket. The E-W-trending leg of the Cust Anticline is related to the E-W-striking Ashley Fault, which has a Holocene trace on the north side of the Ashley River.

### The Ashley Fault

The Ashley Fault is seen as a scarp on the north side of the Ashley river, rejuvenated after trimming by post glacial planation, and with its Holocene eastward emergence tracked by the ages of the succession of channels that it crosses (Sisson et al., 2001). Several paleoseismic trenches were excavated across the Ashley fault, but only one trench produced useful dates, with one immediatedly prior to a calibrated radiocarbon age of 4280 ± 170 years BP and possibly subsequent movements ca. 3530 ± 60 and 3240 ± 70 years BP. The elapsed time since, is consistent with an estimated 3000 year recurrence interval for major uplift events on the Springbank Fault and these structures are closely linked as they form a segment boundary. This is somewhat akin to the recent rupture of the Greendale – Charing Cross fault system.

Several seismic reflection lines cross the Ashley fault, and show that a flower structure has propagated up from a former E-W trending Cretaceous normal fault in basement with associated graben sediments thickening southward. These are now folded and at higher levels in the Tertiary cover, the throw has clearly reversed. Two recent papers address this topic (Ghisetti and Sibson,

2012; Jongens et al., 2012); while there are some differences in interpretation, there are points in common to note with respect to the probable parallels to be drawn with the origin and development of the Greendale Fault, including:

- The inversion is driven by oblique-slip and there is an unknown dextral offset so that sections cannot be balanced, and vertical separation of markers is only a component of net slip.
- The propagation of new faults to the surface is clearly controlled by rejuventated/reversed slip on the basement fault, but shear is spread through several splays so that no single fault necessarily documents the net slip at depth, in terms of measured displacements at the surface.

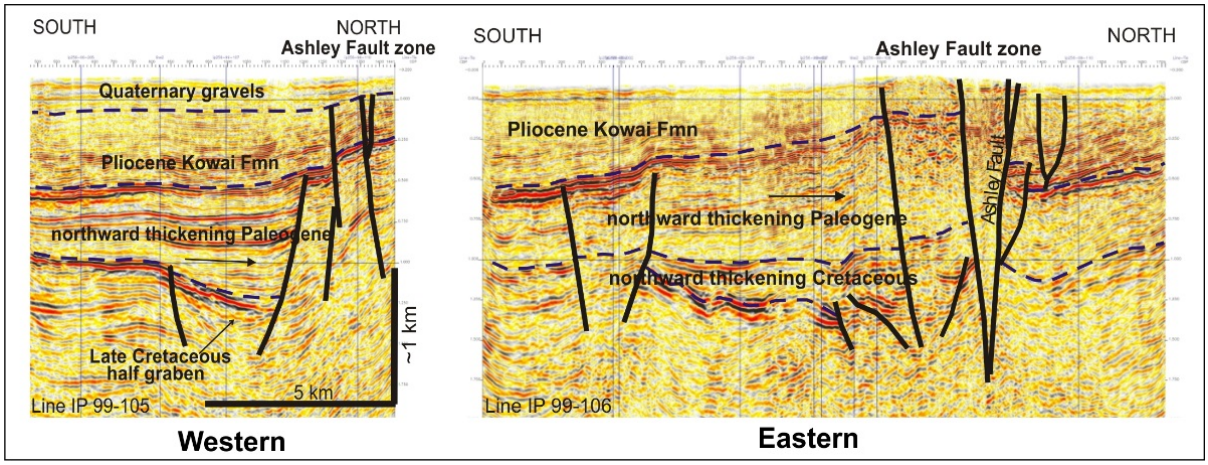


***Figure 12.*** *Industry seismic reflection profiles across the Ashley Fault Zone. The western line crosses the Ashley fault zone where there is no topographic expression of the fault, and shows a Late-Cretaceous/Paleogene half graben on the south side of the fault zone. The eastern line crosses the topographic expression of the Ashley fault zone and clearly shows structural inversion with the north side down (Jongens et al., 2012).*

## The Loburn Fault

The Loburn fault is effectively a fault splay of the Ashley fault zone. It is situated north of the Ashley fault and broadly parallel in its trend. Together, the Ashley and Loburn faults form part of a transpressional inversion structure, expressed by uplift of a low anticlinal ridge between the two faults. The late Quaternary drainage history is strongly influenced by the propagation of both of these structures (Figure 13). The Loburn Fault trace crosses some of the same channel topography, but in this case appears to be re-emerging westward. The thrust-propagated Kowai Anticline terminates at its southern tip against the Loburn fault (Figure 10).

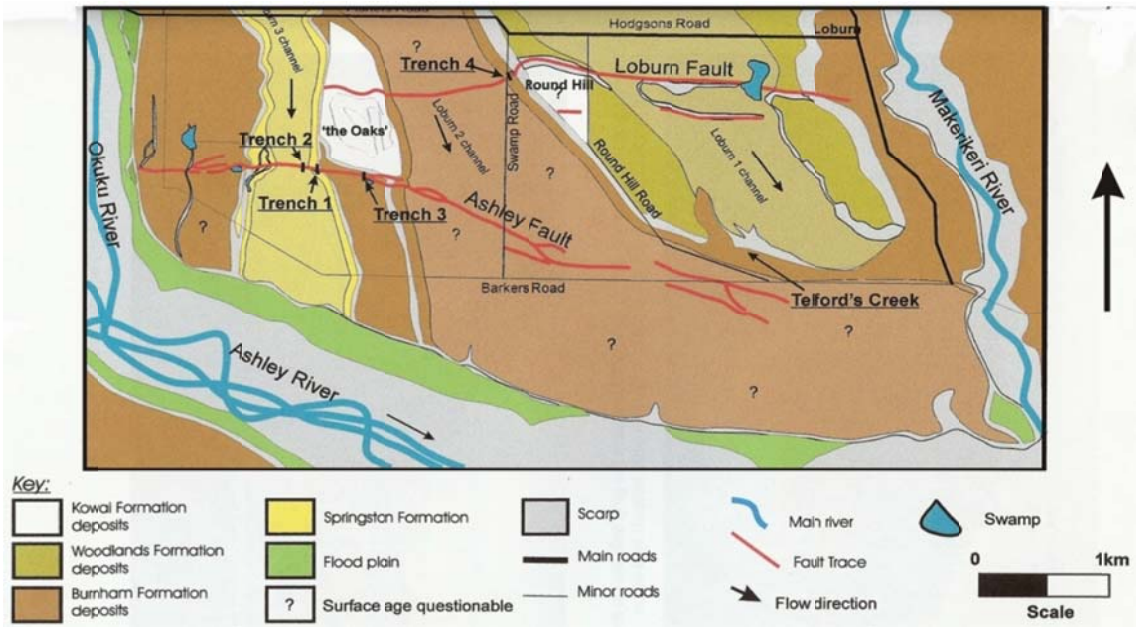


***Figure 13.*** *(Sisson et al., 2001) The Ashley and Loburn Fault traces and their relationship to Quaternary deposits and former channel surfaces. Loburn1 Channel in early Last Glaciation, Loburn 2 in post- LGM, Loburn3 Holocene.*

Between the Ashley and Loburn faults, a pop-up anticline causes the effective surface throw on both faults to reverse along their length. The role of concurrent uplift of this intervening fold, and the more major anticlines to the north and south, appear to control much of the measured slip and is predominantly expressed as uplift near the tips of these faults at the surface. This uplift overprints any strike-slip at depth which would be expected from the orientation of the faults relative to regional stress. By analogy, this is a more evolved structure but comparable in structural style of deformation to the Greendale fault.

### *Points for Discussion in the field:*

- The cause and effect relationship between thrust dominated crustal shortening and reactivation of older faults as tear faults and segment boundaries. Is there potential for slip history on these transecting faults to record adjacent thrust activity and fold growth?
- The relative timing and emergence of these interacting faults during the evolution of blind structures.
- Can the fold geometry and uplift rates of fault propagation anticlines be used to estimate slip rates, likely magnitudes and frequencies on blind faults ?
- How much of the actual slip at seismogenic depths in basement is dissipated into the wall rocks and into backthrusts so that slip rates are underestimated from surface observations of displaced topography over the leading edge of blind thrusts– with implications for paleoseismic studies?

## References

Barnes, P. M., Castellazzi, C., Gorman, A. R., and Wilcox, S., 2011, Submarine faulting beneath Pegasus Bay, offshore Christchurch. Short-term Canterbury Earthquake Recovery Project 2: offshore faults: National Institute of Water and Atmospheric Research.

Barrell, D. J. A., Litchfield, N. J., Townsend, D. B., Quigley, M. C., Van Dissen, R. J., Cox, S. C., Cosgrove, R., Furlong, K., Villamor, P., Begg, J. G., Hemmings-Sykes, S., Jongens, R., Mackenzie, H., Stahl, T., Bilderback, E., Duffy, B., Lang, E. M. W., Nicol, R., Noble, D., and Pedley, K., 2011, Strike-slip ground-surface rupture (Greendale Fault) associated with the 4 September 2010 Darfield earthquake, Canterbury, New Zealand: Quarterly Journal of Engineering Geology and Hydrogeology, v. 44, p. 283-291. DOI:10.1144/1470-9236/11-034

Beavan, J., Motagh, M., Fielding, E., Donnelly, N., and Collett, D., 2012, Fault slip models of the 2010-2011 Canterbury, New Zealand, earthquakes from geodetic data, and observations of post-seismic ground deformation: New Zealand Journal of Geology and Geophysics (Special issue: Canterbury, New Zealand, 2010-2011 earthquake sequence), v. 55, no. 3, p. 207-221. DOI:10.1080/00288306.2012.697472

Beavan, J., Samsonov, S., Denys, P., Sutherland, R., Palmer, N., and Denham, M., 2010, Oblique slip on the Puysegur subduction interface in the 2009 July $M_W$ 7.8 Dusky Sound earthquake from GPS and InSAR observations: implications for the tectonics of southwestern New Zealand: Geophysical Journal International, v. 183, no. 3, p. 1265-1286. DOI:10.1111/j.1365-246X.2010.04798.x

Brown, L. J., Wilson, D. D., Moar, N. T., and Mildenhall, D. C., 1988, Stratigraphy of the late Quaternary deposits of the northern Canterbury Plains, New Zealand: New Zealand Journal of Geology & Geophysics, v. 31, no. 3, p. 305-335

Campbell, J., Pettinga, J., and Jongens, R., 2012, The tectonic and structural setting of the 4th September 2010 Darfield (Canterbury) Earthquake sequence, New Zealand: New Zealand Journal of Geology and Geophysics (Canterbury, New Zealand, 2010-2011 earthquake sequence), v. 55, no. 3, p. 155-168

Cox, S. C., and Barrell, D. J. A., 2007, Geology of the Aoraki area. Institute of Geological and Nuclear Sciences Geological Map 15: GNS Science, scale 1:250,000, 1 sheet & 71 p.

Davy, B., Stagpoole, V., Barker, D., and Yu, J., 2012, Subsurface structure of the Canterbury region interpreted from gravity and aeromagnetic data: New Zealand Journal of Geology and Geophysics, v. 55, no. 3, p. 185-191. DOI:10.1080/00288306.2012.690765

DeMets, C., Gordon, R. G., and Argus, D. F., 2010, Geologically current plate motions: Geophysical Journal International, v. 181, no. 1, p. 1-80

Dorn, C., Green, A. G., Jongens, R., Carpentier, S., Kaiser, A. E., Campbell, F., Horstmeyer, H., Campbell, J., Finnemore, M., and Pettinga, J., 2010, High-resolution seismic images of potentially seismogenic structures beneath the northwest Canterbury Plains, New Zealand: Journal of Geophysical Research B: Solid Earth, v. 115, no. 11. DOI:10.1029/2010JB007459

Duffy, B., Quigley, M. C., Barrell, D., Van Dissen, R., Stahl, T., Leprince, S., McInnes, C., and Bilderback, E., 2013, Fault kinematics and surface deformation across a releasing bend during the 2010 $M_W$ 7.1 Darfield, New Zealand, earthquake revealed by differential LiDAR and cadastral surveying: GSA Bulletin, v. 125, no. 3-4, p. 420-431. DOI:10.1130/B30753.1

Elliott, J. R., Nissen, E. K., England, P. C., Jackson, J. A., Lamb, S., Li, Z., Oehlers, M., and Parsons, B., 2012, Slip in the 2010 and 2011 Canterbury earthquakes, New Zealand: Journal of Geophysical Research, v. 117, no. B3, p. B03401. DOI:10.1029/2011jb008868

Estrada, B., 2003, Seismic hazard associated with the Springbank Fault, North Canterbury Plains [Geology MSc]: University of Canterbury, 193 p.

Forsyth, P. J., Barrell, D. J. A., and Jongens, R., 2008, Geology of the Christchurch area. Institute of Geological and Nuclear Sciences Geological Map 16: GNS Science, 1 sheet + 67 p, scale 1:250,000.

Ghisetti, F. C., and Sibson, R. H., 2012, Compressional reactivation of E-W inherited normal faults in the area of the 2010-2011 Canterbury earthquake sequence: New Zealand Journal of Geology and Geophysics (Special issue: Canterbury, New Zealand, 2010-2011 earthquake sequence), v. 55, no. 3, p. 177-184

Gledhill, K., Ristau, J., Reyners, M., Fry, B., and Holden, C., 2011, The Darfield (Canterbury, New Zealand) Mw 7.1 earthquake of September 2010: a preliminary seismological report: Seismological Research Letters, v. 82, p. 378-386

Gold, R. D., Stephenson, W. J., Odum, J. K., Briggs, R. W., Crone, A. J., and Angster, S. J., 2013, Concealed Quaternary strike-slip fault resolved with airborne lidar and seismic reflection: The Grizzly Valley fault system, northern Walker Lane, California: Journal of Geophysical Research: Solid Earth, v. 118, no. 7, p. 3753-3766. DOI:10.1002/jgrb.50238

Holbrook, J., and Schumm, S. A., 1999, Geomorphic and sedimentary response of rivers to tectonic deformation: A brief review and critique of a tool for recognizing subtle epeirogenic deformation in modern and ancient settings: Tectonophysics, v. 305, no. 1-3, p. 287-306

Hudnut, K. W., Borsa, A., Glennie, C., and Minster, J.-B., 2002, High-Resolution topography along surface rupture of the 16 October 1999 Hector Mine, California, Earthquake ($M_W$ 7.1) from airborne laser swath mapping: Bulletin of the Seismological Society of America, v. 92, no. 4, p. 1570-1576

Jongens, R., Barrell, D. J. A., Campbell, J. K., and Pettinga, J. R., 2012, Faulting and folding beneath the Canterbury Plains identified prior to the 2010 emergence of the Greendale Fault: New Zealand Journal of Geology and Geophysics (Special issue: Canterbury, New Zealand, 2010-2011 earthquake sequence), v. 55, no. 3, p. 169-176

Jongens, R., Pettinga, J., and Campbell, J., 1999, Stratigraphic and structural overview of the onshore Canterbury Basin: North Canterbury to the Rangitata River. Report prepared for Indo-Pacific Energy Ltd.: University of Canterbury.

Kaiser, A., Dellow, G., Denys, P., Fielding, E., Fry, B., Gerstenberger, M., Langridge, R., Massey, C., Motagh, M., Pondard, N., McVerry, G., Holden, C., Ristau, J., Stirling, M., Thomas, J., Uma, S. R., Zhao, J., Beavan, J., Beetham, D., Benites, R., Celentano, A., Collett, D., Cousins, J., and Cubrinovski, M., 2012, The M-w 6.2 Christchurch earthquake of February 2011: preliminary report: New Zealand Journal of Geology & Geophysics, v. 55, no. 1, p. 67-90. DOI:10.1080/00288306.2011.641182

Little, T. A., and Jones, A., 1998, Seven million years of strike-slip and related off-fault deformation, northeastern Marlborough fault system, South Island, New Zealand: Tectonics, v. 17, no. 2, p. 285-302. DOI:10.1029/97tc03148

Nicol, A., 1993, Haumurian (c.66-80 Ma) half-graben development and deformation, mid Waipara, north Canterbury, New Zealand: New Zealand Journal of Geology & Geophysics, v. 36, no. 1, p. 127-130

Nicol, A., and Campbell, J. K., 2001, The impact of episodic fault-related folding on late holocene degradation terraces along Waipara River, New Zealand: New Zealand Journal of Geology and Geophysics, v. 44, no. 1, p. 145-155

Price, E. J., and Burgmann, R., 2002, Interactions between the Landers and Hector Mine, California, earthquakes from space geodesy, boundary element modeling, and time-dependent friction: Bulletin of the Seismological Society of America, v. 92, no. 4, p. 1450-1469

Quigley, M. C., Van Dissen, R., Litchfield, N., Villamor, P., Duffy, B., Barrell, D., Furlong, K., Stahl, T., Bilderback, E., and Noble, D., 2012, Surface rupture during the 2010 $M_W$ 7.1 Darfield (Canterbury) earthquake: implications for fault rupture dynamics and seismic-hazard analysis: Geology, v. 40, no. 1, p. 55-58. DOI:10.1130/G32528.1

Reigber, C., Xia, Y., Michel, G. W., Klotz, J., and Angermann, D., The Antofagasta 1995 earthquake: Crustal deformation pattern as observed by GPS and D-INSAR, *in* Proceedings Proceedings of the 3rd ERS Symposium on Space at the Service of Our Environment, , Florence, Italy, 14-21 March 1997, European Space Agency, p. 507-513.

Sibson, R., Ghisetti, F., and Ristau, J., 2011, Stress control of an evolving strike-slip fault system during the 2010-2011 Canterbury, New Zealand, earthquake sequence: Seismological Research Letters, v. 82, no. 6, p. 824-832

Sisson, R., Campbell, J., Pettinga, J., and Milner, D., 2001, Paleoseismicity of the Ashley and Loburn Faults, North Canterbury, New Zealand: Earthquake Commission Research Foundation report 97/237

Syracuse, E. M., Thurber, C. H., Rawles, C. J., Savage, M. K., and Bannister, S., 2013, High-resolution relocation of aftershocks of the Mw 7.1 Darfield, New Zealand, earthquake and implications for fault activity: Journal of Geophysical Research: Solid Earth, p. n/a-n/a. DOI:10.1002/jgrb.50301

Wallace, L. M., Beavan, J., McCaffrey, R., Berryman, K., and Denys, P., 2007, Balancing the plate motion budget in the South Island, New Zealand using GPS, geological and seismological datas: Geophysical Journal International, v. 168, no. 1, p. 332-352

Wood, R. A., and Herzer, R. H., 1993, The Chatham Rise, New Zealand, *in* Ballance, P. F., ed., South Pacific sedimentary basins: Amsterdam, Elsevier Science Publishers, p. 329-349.